# INTERNATIONAL SOCIETY FOR SOIL MECHANICS AND GEOTECHNICAL ENGINEERING



This paper was downloaded from the Online Library of the International Society for Soil Mechanics and Geotechnical Engineering (ISSMGE). The library is available here:

https://www.issmge.org/publications/online-library

This is an open-access database that archives thousands of papers published under the Auspices of the ISSMGE and maintained by the Innovation and Development Committee of ISSMGE.

# Seismic Site Classification

Ramon Verdugo CMGI Ltda., Santiago, Chile



#### **ABSTRACT**

The economic losses left by large recent earthquakes are still considerable, and modern society is wanting not only life protection; it is also demanding that buildings can be immediately occupied after a strong earthquake. The performance-based seismic design allows engineers to design structures with a desired seismic performance for a specified level of hazard. This requires a high standard in the different items involved in the seismic design. One of the key factors is associated with the seismic loads, which are strongly dependent on the local ground conditions. Accordingly, an alternative seismic site classification is proposed, which is based on two dynamic parameters of the ground: the equivalent shear wave velocity, V<sub>S30-E</sub>, that reproduces the dynamic lateral stiffness of the upper 30 m of the ground, and the predominant period of the site, which is proposed to be estimated via the H/V spectral ratio of ambient vibration measurements. All the details of this site classification are explained in the paper.

### 1 INTRODUCTION

It is an empirical fact that recent large and medium earthquakes have caused significant economic losses. An important part of these losses is attributed to the severe damages suffered by buildings (residential, commercial, industrial, governmental, educational, cultural, hospital, etc.), infrastructure and structures of the production sector. For example, in Table 1 the estimated direct economic losses of the latest earthquakes are presented (Data from USGS 2011; Kajitani et al. 2013; Horspool et al. 2016; Aon Benfield 2015 and Senplades 2016).

Table 1. Economic loss of recent earthquakes

Earthquake	Dater	Mw	Direct Loss (billion US\$)
Maule, Chile	Febru. 2010	8.8	30
Tohoku, Japan	March, 2011	9.0	211
Christchurch, NZ	Febru. 2011	6.3	40
Nepal	April, 2015	7.8	10
Muisne, Ecuador	April, 2016	7.8	3

It can be observed that in spite of the tremendous advances in the field of earthquake engineering, economic losses are still considerable, far from any socio-economically satisfactory standard. In the particular case of Tohoku Earthquake, the cost is substantially high due to the damages caused by the tsunami. In any case, modern society is wanting not only life protection; it demands that buildings can be occupied and function following a strong earthquake. This also means that water, electricity, gas, and other services have to be operational as well. Therefore, the challenge is to reduce the tremendous economic impact that earthquakes still have on society, and accordingly, resilience and reliability of structures is an important issue (Cimellaro, 2017).

According to FEMA (2012), one of the most promising tools that can be used to reduce the damage and losses

resulting from an earthquake, or other similar disaster, is performance-based seismic design (PBSD). This design methodology allows engineers to design structures and nonstructural components with a desired seismic performance for a specified level of hazard. The philosophy is to accomplish a reliable structure design meeting performance objectives (Priestley, 2000)

To achieve these goals, among other factors, the ground conditions have to be identified in order to estimate the seismic loads.

The effect of local soil conditions on ground surface motions has been widely recognized from both theoretical and empirical points of view. Under large earthquakes, it has been observed that, in general, structures placed on rock outcrops and stiff soil deposits consisting of dense granular materials behave well with no damage or only with some minor negative seismic effects. Conversely, when the soil conditions are associated with soft materials (as for example, saturated clayey or deep deposits of sandy soils), it is common the occurrence of severe damages, and even the collapse of structures when subjected to seismic loads (Montessus de Ballore, 1911; Watanabe et al. 1960; Borcherdt, 1970; Seed et al. 1988). Hence, the seismic site classification is an important issue that permits the appropriate estimation of the seismic loads that have to be used in the analysis associated with the performance-based seismic design. Consequently, in this article the seismic classification of a site is addressed and an alternative procedure is proposed.

# 2 PERFORMANCE-BASED SEISMIC DESIGN

Historically, seismic design has focused on providing resistance to the structural components of the structures. However, it is well recognized that this approach by itself does not guarantee successful seismic behavior of the structure. For example, it is well known that it is inadequate to provide higher resistance to the beams than to the columns in a frame structure; under severe seismic loadings a better response is expected if plastic

hinges are developed in the beams rather than in the columns. This example suggests that, conceptually, an appropriate seismic design should identify the overall performance of the structure when subjected to strong earthquakes. Going further, achievement of specific results can be established and then included as part of the design process. Accordingly, the seismic design has moved from resistance criteria to performance objectives that have to be satisfied by the structure during and after earthquakes.

Taking into account that recent earthquakes have continued causing significant economic losses, earthquake engineering is forced to design for damage control, functionality and serviceability, maintaining and improving the life-safety as a primary requirement. Accordingly, PBSD would be the solution to produce structures with a predictable seismic behavior.

PBSD has the advantage of considering both the level of ground shaking and the associated level of performance. This means that for different levels of shaking considered as input motion, different target performance levels can be specified or requested. Therefore, protection levels, or performance levels, in seismic design against different seismic scenarios can be introduced; for example as presented in Table 2.

Table 2. Performance levels

Performance Level	Description
Continued Operation	Structural & nonstructural components response essentially with no damage.
Immediate	Structural elements with no damage.
Occupancy	Non-structural components may not be functional.
Life Safety	Noticeable damage to the structure may occur and repair may not be economically feasible.
	The risk of life-threatening injury has to be low.
Collapse Prevention	Severe structure damage could occur, but the structure does not collapse.
	Significant risk of injury exists.

On the other hand, the different seismic scenarios, or seismic hazard levels, to be considered in seismic design are associated with their recurrence interval and corresponding probability of occurrence. Table 3 indicates the most common hazard levels for building and industrial facilities.

Service Level Earthquake (SLE) represents the ground motions that are estimated to occur most frequently (50% probability of exceedance in 50 years), and therefore, no damage is expected in the structures. For industrial facilities, the Operating Basis Earthquake (OBE) is defined as the event that can occur during the design life of the facility (10% probability of exceedance in 50 years), accordingly, little to no damage is expected, so the operation can re-start immediately or a short time after the earthquake. In the case of buildings, it corresponds to

the Design-Basis Earthquake. The maximum considered earthquake (MCE) is associated with 2% probability of being exceeded in 50 years, or an average return period of 2475 years. In the case of buildings, severe structure damage could occur, but the structure will not collapse, although significant risk of injury exists. The Safe Shutdown Earthquake is applied in seismic design of critical structures (for example, chemical industries, Liquefied Natural Gas industries, power plants and nuclear facilities, among others). It is defined as the maximum earthquake potential for which certain structures, systems, and components, important to safety, are designed to sustain and remain functional.

Table 3. Seismic hazard levels.

Frequency	Probability of exceedance in 50 years	Mean return Period (years)	Terminology
Frequent	50%	72	Service-Level Earthquake (SLE)
Rare	10%	475	Design-Basis Earthquake or Operating Basis Earthquake (OBE)
Very rare	5%	975	Basic Safety Earthquake (BSE)
Extremely rare	2%	2475	Maximum Considered Earthquake (MCE)
Excessively rare	1%	4975	Safe Shutdown Earthquake (SSE)

The PBSD philosophy uses a probabilistic approach to define the seismic hazard levels. However, it is possible to use a deterministic seismic hazard analysis to establish the largest earthquake magnitude for a particular seismic source, which is referred to as the Maximum Credible Earthquake, also identified as MCE.

In the framework of PBSD, it is apparent that the input loads in any structure analysis are the basis to obtain a realistic and reliable result. Thus, the proper estimation of the seismic loads to which the structure will be subjected turns out to be a fundamental issue in the analysis. This is especially important, when applying the PBSD method, where pre-established seismic performance levels have to be achieved.

The seismic analysis of structures can be done using modal spectral analysis, which requires a spectrum associated with the considered seismic action. Besides the seismic hazard level, the considered spectrum is strongly dependent of the ground conditions, or geotechnical-geological characteristics of the site. Different local site conditions may generate quite different spectral shapes, which may change drastically the seismic loads applied on the structure.

According to the philosophy of PBSD explained above, it is essential to keep in mind that PBSD requires that each of the steps associated with the analyses be performed with the lowest level of uncertainty that the profession may guarantee. In this respect, it is evident that the assessment of the seismic loads to be applied to the analyzed structures is a fundamental issue. Nonetheless, this is probably one of the weakest points involved in the actual application of PBSD. Besides the seismologic study for establishing the earthquake characteristics of the different seismic hazard levels and the engineering decision to adopt a particular seismic scenario, the resulting seismic loads are strongly dependent on the local geological-geotechnical conditions of the ground where the structure will be located (Dobry et al. 2000; Pitilakis et al. 2004). This phenomenon is commonly referred to as a site effect. Even though this is a well-known fact, the seismic site classifications adopted by different seismic provisions suffer from a rather simplistic methodology that in many cases can wrongly estimate the design spectra, and consequently, the acting seismic forces can be seriously underestimated. If this happens, the PBSD loses all its capability for predicting the structure response under different seismic hazard levels. Thus, the site effect and therefore, the site classification are important issues that are addressed by the author in this paper.

### 3 SITE EFFECT - EMPIRICAL EVIDENCE

The empirical evidence left by large earthquakes clearly shows that the intensity of the motion developed at the ground surface is strongly controlled by the type of soil and thickness of the sediments. A remarkable case of amplification is the one observed during the 1985 Mexico City earthquake of Magnitude 8.1, where the shaking was amplified by a factor of 20, or even more, on sites consisting of deep soil deposits of soft fines materials (Celebi et al. 1987; Singh et al. 1993). On the other hand, rock outcrops and stiff soil deposits have shown a significant reduction in the shaking intensity (Montessus de Ballore, 1911; Watanabe et al. 1960; Borcherdt, 1970; Seed et al. 1988). An interesting experience that shows the site effect took place during the 1906 Valparaiso Earthquake of Magnitude, Mw = 8.2. This strong ground motion occurred approximately 4 months after the San Francisco Earthquake, where similar site effects were observed (Borcherdt et al. 1976). Figure 1 shows the general geology of Valparaíso, which basically consists of a massive rock outcrop of the Coastal Range and a rather small plane area consisting mainly of medium to dense sandy soils. A borehole performed near to the National Congress (Figure 2) found bedrock at a depth of 57 m.

Among the few buildings that underwent minor damages during the 1906 Valparaiso Earthquake are Aduana and Palacio Lyon. The Aduana building is located on rock outcrop and Palacio Lyon is quite close to the rock outcrop, so the bedrock is expected a few meters below this building, as indicated in Figure 2.

These two historical buildings still exist today as shown in the photos in Figure 3, which means that they have also responded appropriately to the series of shakes

that occurred later, especially during the 1985 (Mw = 7.8) and 2010 (Mw = 8.8) earthquakes.

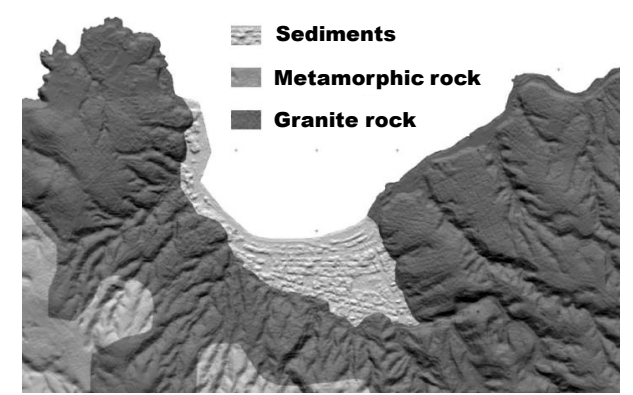


Figure 1. General geology of Valparaiso (with slight modification from Indirli et al. 2010)



Figure 2. Location of emblematic buildings that collapsed during the 1906 Earthquake and buildings that exist even today.



Figure 3. Aduana (left) a Palacio Lyon (right) buildings founded on bedrock or very near to it. Old and recent photos.

On the other hand, severe destruction of buildings located in the soil deposit was reported. Two emblematic building, Teatro Victoria (built in 1886) and Iglesia de la Merced (built in 1893), collapsed during the earthquake, as shown in the photos of Figure 4 (Rodriguez et al. 1906).

Henriquez (1907) and Montessus de Ballore (1911) concluded that geological conditions are fundamental in the observed damage. They reported that buildings placed on soil deposits that suffered heavy damage, while

structures placed on hills (rock outcrops) experienced no damage, or it was negligible. This is confirmed in the photo of Figure 5, which shows refugees in the hilly area and the undamaged buildings that amazingly remained in this area.



Figure 4. De la Merced Church and Victoria Theater before and after de 1906 Earthquake.



Figure 5. Hilly area with undamaged buildings.

Conversely, the photos of Figure 6 tell of the total destruction that occurred in the area of soft ground. This important lesson of significantly better seismic performance of structures founded on rock or competent soils has been systematically observed in large earthquakes. This fact has important practical consequences, since it allows the seismic response of highly competent geotechnical ground to be assessed differently from sites with regular to low geotechnical properties.



Figure 6. Total destruction in the area of ground consisting of a sandy soil deposit (intersection of Blanco and Edwards streets).

# 4 SITE CHARACTERIZATION

Analyzing 104 acceleration records with PGA greater than 0.05g, Seed and co-workers (Seed et al. 1976) proposed normalized spectral forms considering the site-dependent ground motion characteristics. In Figure 7 the mean spectra categories, defined for different site conditions, are shown. The differences of these spectral shapes are evident, being very significant for periods greater than 0.5 sec, where soil deposits consisting of soft to medium clays and sands present the higher spectral amplification. Conversely, for periods below 0.4 sec, the higher spectral amplification is observed in deposits consisting of stiffer soils. These results were also reproduced by other studies (Mohraz, 1976), and then incorporated in the ATC 1978, using idealized spectral shapes considering three site conditions, as shown in Figure 8, where the concept of Site Class, or Soil Type, for grouping sites with similar geotechnical-geological conditions was introduced.

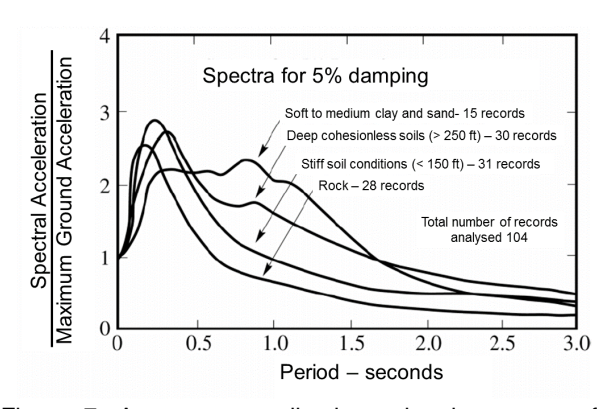


Figure 7. Average normalized acceleration spectra for different site conditions (Seed et al. 1976).

Each soil type would develop the same seismic amplification, which is assigned through a specific design response spectrum. Site Class is determined based on the properties of the soils existing in the top 30 m of the ground. However, it is apparent that from a seismic point of view, deep soil deposits cannot be characterized considering only the upper 30 m of the ground. This is revisited later.

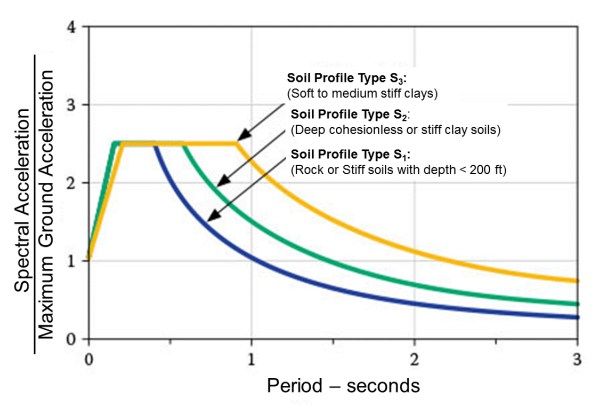


Figure 8. Spectral shapes proposed by ATC 3 (1978) for three different soil types codes.

An attempt to classify the geotechnical site conditions unambiguously was introduced by Borcherdt and Glassmoyer (1992) and Borcherdt (1994), by means of the representative shear wave velocity,  $V_{\rm S30}$ , of the upper 30 m of the soil profile. The value of  $V_{\rm S30}$  is such that reproduces the vertical travel time of the shear wave propagating throughout the top 30 m of the ground. Accordingly, the expression for its evaluation is:

$$V_{S30} = \frac{\sum_{i=1}^{n} h_{i}}{\sum_{i=1}^{n} h_{i} / V_{Si}}$$
[1]

Where, n corresponds to the number of layers identified in the upper 30 m of the ground. The terms hi and Vsi represent the thickness and shear wave velocity, respectively, of the layer i.

The decision of adopting a depth of 30 m was somewhat arbitrary and is mainly associated with practical reasons; it corresponds to the typical exploration depth of geotechnical boreholes. Although in some soil profiles this parameter may lead to incorrect assessments of the site amplification, most of the code provisions for civil structures have adopted it as the main parameter for site classification.

The International Building Code (IBC) and ASCE7 have established Site Class A to F (Table 4).

Site Class A, hard rock, associated with a shear wave velocity,  $V_{\rm S30} > 1500\,$  m/s, corresponds to the most competent geotechnical material. This type of rock could be found to the east of Rocky Mountains. In regions of high seismicity, this type of rock is unusual, and therefore, other seismic codes do not consider this type of rock. In contrast, Site Class B, defined as a rock with  $V_{\rm S30} > 750\,$  m/s, is a common rock outcrop in seismic regions. At the other extreme, site class F corresponds to sites with special soil conditions such as liquefiable soils, collapsible weakly cemented soils, sensitive clays, highly organic clays, very high plasticity clays and very thick soft clays. As a result, Site Class F requires special analyses.

It is important to observe that although the main parameter to classify a site is V<sub>S30</sub>, strength parameters

such as penetration resistance (N-SPT) and undrained shear strength ( $S_u$ ), of the upper 30 m of the ground, can also be used.

Table 4. Site Classification ASCE7-10

Site Class	$\overline{V_{S30}}$ (m/s)	$\overline{N}$ or $\overline{N_{ch}}$	$\overline{S_u}$ (kPa)
A. Hard rock	> 1500	NA	NA
B. Rock	750 to 1500	NA	NA
C. Very dense soil and soft rock	360 to 750	> 50	> 96
D. Stiff soil	180 to 360	15 to 50	48 to 96
E. Soft clay soil (*)	< 180	< 15	< 48
F. Soils requiring site response analysis			

 $(1 \text{ ft/s} = 0.3048 \text{ m/s}; 1 \text{ lb/ft}^2 = 0.0479 \text{ kN/m}^2)$ 

(\*): Any profile with more than 3 m of soil having the following characteristics: Plasticity index PI >20; Moisture content w  $\geq$  40%; Undrained shear strength,  $S_u < 24$  kPa.

Conceptually, the seismic amplification phenomenon, like any other dynamic behavior that is far from failure, requires for its analysis material parameters associated with stiffness, damping and mass. Therefore, strength parameters are not the most suitable ones for site characterization, and their use should only be complementary.

It is interesting to note that the ASCE7-10 gives two options for those situations with a lack of information:

- "Where site-specific data are not available to a depth of 100 ft (30 m), appropriate soil properties are permitted to be estimated by the registered design professional preparing the soil investigation report based on known geologic conditions."
- Where the soil properties are not known in sufficient detail to determine the site class, Site Class D shall be used unless the authority having jurisdiction or geotechnical data determine Site Class E or F soils are present at the site.

These options seem rational and useful when the site is somehow isolated (far from urban areas) and the projected structures are rather small, so any overdesign does not affect significantly the cost of the project.

Another valuable code is the Eurocode 8 (EC8), where five Ground Types, identified as A, B, C, D and E have been established (Table 5).

Each Ground Type is defined according to the resulting value of  $V_{\rm S30}$ . However, when shear wave velocities are not available, resistance parameters such as N-SPT and  $S_{\rm u}$  may be used to select the

corresponding Ground Type. It is considered important to comment again that resistance parameters are not the best option to characterize a site from its expected dynamic response.

Table 5. Ground Types Eurocode 8

Ground	Stratigraphic	V <sub>S30</sub>	N <sub>SPT</sub>	S <sub>U</sub>
Туре	profile	(m/s)	01 1	(kPa)
Α	Rock or other rock-like geological formation.	> 800	-	-
В	Deposits of very dense sand, gravel, or very stiff clay, at least several tens of meters in thickness.	360-800	> 50	> 250
С	Deep deposits of dense or medium-dense sand, gravel or stiff clay with thickness from several tens to many hundreds of meters.	180-360	15-50	70-250
D	Deposits of loose-to- medium cohesionless soil, or of predominantly soft- to-firm cohesive soil.	< 180	< 15	< 70
E	A soil profile consisting of a surface alluvium layer with $V_{\rm S}$ values of type C or D and thickness varying between 5 – 20 m, underlain by stiffer material with $V_{\rm S}{>}800$ m/s.			
S <sub>1</sub>	Deposits consisting, or containing a layer at least 10 m thick, of soft clays/silts with a high plasticity index (PI>40) and high water content.	< 100	-	10-20
S <sub>2</sub>	Deposits of liquefiable soils, sensitive clays, or any other soil profile not included in types A, E, S <sub>1</sub> .			

In the EC8, the Ground Type A represents rock outcrops with  $V_{\rm S30}$  > 800 m/s, which is similar to Site Class B in the ASCE7-10.

In particular, the Ground Type E is introduced, which is defined as a surface alluvium material with  $V_S < 360 \text{ m/s}$  and a thickness less than 20 m, underlain by rock ( $V_S > 800 \text{ m/s}$ ). This singular condition is associated with high impedance ratio that is expected to amplify the seismic response. Similar to IBC and ASCE7, the EC8 has defined singular Ground Types (S1 and S2), which basically consist of soil deposits that require special analyses, for example, fines soils with high plasticity and high water content, liquefiable soils and sensitive clays.

Following similar concepts, the Chilean code DS-61 (2011), basically defines six Soil Types identified from A to E according to the shear wave velocity of the upper 30 m,  $V_{\rm S30}$  (Table 6). This code requests as primary parameter  $V_{\rm S30}$ , and as a complement the N-SPT for sandy soils and  $S_{\rm u}$  for fines soils. Additionally to the six Soil Types, the Chilean code has grouped as Site Type F

all those soil deposits considered special or unique, for example, liquefiable soil, organics, fines soils of high plasticity and highly sensitive soils, etc.. Accordingly, these soils (Soil Type F) require special dynamic analysis.

Table 6. Soil Types of Chilean Code, DS-61.

Soil Type	V <sub>S30</sub> (m/s)	RQD (%)	q <sub>u</sub> (MPa)	N <sub>1</sub>	S <sub>∪</sub> (MPa)
A Rock, cemented soils	≥ 900	≥ 50	≥ 10	-	
B Soft or fractured rock, very dense soils	≥ 500		≥ 0.4	≥ 50	
C Dense, firm soils	≥ 350		≥ 0.3	≥ 40	
<b>D</b> Medium-dense or medium-firm soils	≥ 180			≥ 30	≥ 0.05
E Soils of medium consistency	< 180			≥ 20	< 0.05
F Special soils	-				
		0			

N<sub>1</sub>: Normalized N-SPT at 1 kg/cm<sup>2</sup>; q<sub>u</sub>: Unconfined strength

These three seismic codes (ASCE7-10, EC8 and DS-61) establish geological-geotechnical conditions of the upper 30 m of the ground in order to group the sites with similar expected seismic response. The identification of each site class according to  $V_{\text{S30}}$  is summarized in Figure 9. It can be observed that these three codes use similar values of V<sub>S30</sub> to separate the different Soil Type, or Site Classes. The exception is the Soil Type C defined in the Chilean code that was introduced to generate a smoother transition from very dense granular material to medium dense sands and stiff clays. Another difference is the frontier between Soil Type A (rock and cemented soils) and Soil Type B (very dense soils) is stablished at  $V_{S30} = 900$  m/s, because to the west of Los Andes Range there are several non-cemented dense gravelly soil deposits with shear wave velocity in the order of 800 m/s.

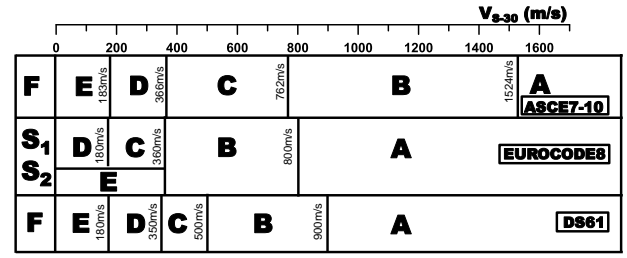


Figure 9. Boundaries of Soil Types in terms of V<sub>S30</sub>

The above-described methods to assess the site classification present an inherent weakness; they rest on the properties of the top 30 m of the ground, neglecting the effects of both the properties of the soils below a depth of 30 m and the total depth of the soil layers.

On the other hand, the Japanese provisions for seismic soil classification consider only three site conditions, identified as soil profile types I, II, and III, which are basically representing hard, medium and soft soil deposits. In particular, the Highway Bridge Design

Code considers the ground period,  $T_G$ , which is calculated as follows:

$$T_G = 4\sum_{i=1}^{n} \frac{h_i}{V_{Si}}$$
 [2]

Where, i represents the i-soil layer defined from the ground surface down to the engineering bedrock, and hi and  $V_{S\,i}$  correspond to its respective thickness and shear wave velocity. The engineering base depends on professional judgement, for instance N-SPT  $\geq$  50 blows, or shear wave velocity greater than 400 m/s (Towhata 2016). The description and requested values of  $T_G$  for each of the Soil Types are indicated in Table 7.

Table 7. Soil Types Japanese Highway Bridge Design

Soil	Ground	T <sub>G</sub>
Profile	characteristics	(s)
Type I (Hard soil)	Rock, hard sandy gravel or gravel, and other soils mainly consisting of tertiary or older layers.	< 0.2
Type II	Other than Type II or III	0.2 - 0.6
Type III (Soft soils)	Alluvium mainly consisting of organic, mud, or other soft soils.	> 0.6

As can be observed, the Japanese provisions associated with the site classification differ from the previous described methods. The Japanese procedure does not use the shear wave velocity of the top 30 m,  $V_{\rm S30}$ , of the ground; instead of this, it uses the ground period,  $T_{\rm G}$ . Besides, it attempts to include the complete soil deposit introducing the concept of engineering bedrock and it considers coarsely only three soil profiles. Nevertheless, there exist complex soil deposits consisting of several layers of different materials, in which case the site classification may be oversimplified.

# 5 PARAMETERS FOR A SITE CLASSIFICATION

Although there are soil deposits with a thickness equal to or less than 30 m, in general, soil deposits are deeper than 30 m. Therefore, any site classification that by definition only takes into account the soil properties of the top 30 m, most probably would wrongly evaluate the seismic response of a site, especially if soil layers with different properties are present below 30 m. However, it is important to recognize that for ordinary projects a geotechnical exploration down to the bedrock would not be practical, particularly in deep soil deposit.

In spite of that, it is important to realize that the upper 30 m of ground also plays a role in the resulting seismic response at the ground surface. For example, the recorded accelerations in the LLolleo down-hole array (Verdugo 2009) show systematically that the seismic amplification is developed mainly in the upper 20-30 m of the ground. Therefore, characterization of the upper 30 m of a site provides valuable information about the amplification phenomenon, but is not sufficient.

Therefore, the main issue to improve the current state of site classification is to obtain a complementary parameter that provides fundamental information of the entire soil deposit (from the surface down to the bedrock), influencing its seismic response at the surface. Additionally, a practical requirement for this parameter is that it must be economically attractive. These requirements are fulfilled by the predominant period of a site, which can be estimated through the measurement of ambient vibrations and calculation of the H/V spectral ratio (Nakamura 1989; Koller et al. 2004; Konno et al. 1998; Lachet et al, 1994; Lermo et al, 1993; Pastén 2007; Verdugo et al. 2008). This procedure, also referred to as Nakamura's method, is broadly used in several European and Asian countries. However, it is not used all around the world. Because of this, empirical evidence to confirm its capability to estimate the predominant period of a site is presented.

Returning to the characterization of the upper 30 m of the ground and recognizing that site amplification is essentially a dynamic phenomenon, it is considered appropriate to use a stiffness parameter rather than a strength parameter. In this context, the shear wave velocity is the most suitable parameter to characterize the top 30 m of a site. However, it is necessary to review the applicability of  $V_{\rm S30}$ , because for a stratified soil structure it does not reflect the resulting stiffness, it just corresponds to the shear wave velocity with the same travel time as the actual soil. Accordingly, to characterize the upper 30 m of a site, the shear wave,  $V_{\rm S30-E}$ , that reproduces the shear stiffness of the top 30 m of the ground is proposed.

It is important to emphasize that the use of strength parameters to predict the seismic response is inadequate. In the context of dynamic analysis, strength parameters of the existing soils should be considered only as index values that, in general terms, are related to the stiffness of the site.

Consequently, to characterize a site for an estimation of its expected seismic response at the ground surface, the following two parameters are proposed:

- The equivalent shear wave velocity of the upper 30 m of the site that represents the shear stiffness of these upper 30 m.
- The predominant period of the site evaluated through ambient vibrations applying the H/V spectral ratio (HVSR)

The estimation of these parameters and the proposed methodology of how to combine these two parameters for site classification is presented below.

# 6 ESTIMATION OF THE PREDOMINANT PERIOD OF A SITE

To verify the capability of the HVSR for assessing the predominant period of a site, the available acceleration records of two of the recent large earthquakes that occurred in Chile are analyzed. A brief description of these earthquakes is presented as follows.

Maule Earthquake: It hit the Central-South region of Chile on February 27, 2010 with a Magnitude Mw = 8.8. This earthquake corresponds to a thrust-faulting type event associated with the subduction seismic environment caused by the collision between the Nazca and South American tectonic plates. The rupture zone responsible for this quake covered a rectangular area of approximately 550 km by 170 km, at an average depth of 35 km. A total number of 36 seismic stations located in the most affected area recorded the acceleration time histories on rock outcrops and soil deposits of different geotechnical characteristics. The maximum PGA recorded on a rock outcrop was 0.32g in Santa Lucía Hill in Santiago, whereas the maximum PGA recorded on a soil deposit reached a value 0.94g in Angol city, located close to the south end of the rupture zone. The recorded horizontal peak accelerations are presented in Figure 10 (Verdugo et al, 2015). The rectangular area enclosed by a broken line corresponds to the rupture zone.

Illapel Earthquake: On September 16, 2015, the Illapel Earthquake, of magnitude Mw = 8.3, hit the Central-Noth region of Chile. The rupture plane occurred at a depth of 23 km, according to the National Seismological Center (Barrientos 2015). The highest horizontal acceleration recorded was 0.83g (station C110, component E-W). The records available with horizontal maximum accelerations equal to or greater than 0.2g were analyzed, which correspond to eight stations as shown in Table 8.

Table 8. Stations with recorded PGA greater than 0.2g. Illapel Earthquake of Mw = 8.3.

Station	a <sub>max</sub> (g) N-S	a <sub>max</sub> (g) E-W	a <sub>max</sub> (g) Vert.
C110	0.71	0.83	0.48
C180	0.51	0.48	0.23
C260	0.23	0.36	0.13
C003	0.29	0.35	0.20
G004	0.34	0.24	0.16
C100	0.29	0.31	0.19
C140	0.18	0.30	0.16
C200	0.25	0.26	0.18

In the case of Maule Earthquake, the available information of HVSR obtained using ambient vibrations measured near the seismic stations was used to obtain the predominant period of the station sites. However, this information is not available yet in the case of the stations that recorded the Illapel Earthquake.

Nevertheless, in these stations, besides the Illapel Earthquakes, several small earthquakes were also recorded, which have been used as microtremors to evaluate the HVSR and then the predominant periods of the sites where the stations are located.

On the other hand, the psedo-acceleration response spectra evaluated from the recorded acceleration time histories provide information about the frequency content of the signal, and therefore, it is possible to obtain the predominant period of the sites where the stations are located. Nevertheless, depending on the geotechnical and

geological characteristics of the site, it is possible to have spectra with several peaks of similar amplitudes being difficult to identify the predominant period. Thus, a complementary tool to estimate the predominant period from the recorded acceleration time histories is proposed.



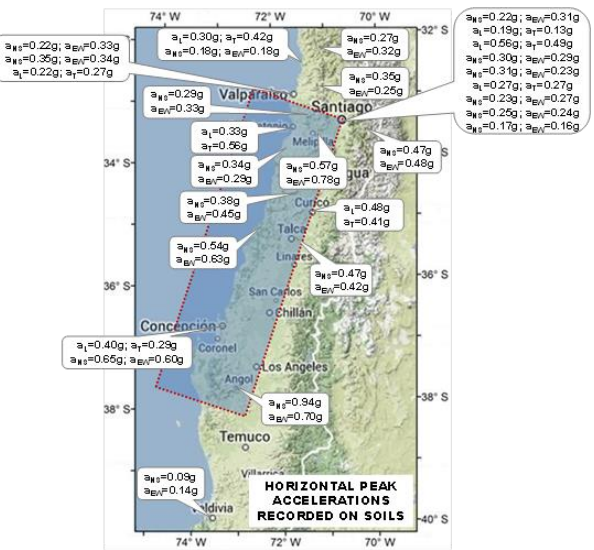


Figure 10. Horizontal peak acceleration recorded on rock outcrops and soil deposits. 2010 Maule Earthquake.

The psedo-acceleration response spectrum is built taking the peak acceleration of the response of a single degree of freedom (SDOF) oscillator for each natural frequency or period considered in the SDOF.

Instead of using the peak acceleration of each response, it is proposed to evaluate the energy of each response. If the response of a SDOF of frequency  $\omega$  in terms of acceleration is  $a_{\omega}(t)$ , the energy,  $E_{\omega}$ , of this response is:

$$E_{\omega} = \int_{0}^{t_f} [a_{\omega}(t)]^2 dt$$
 [3]

Where,  $t_{\rm f}$  is the duration of the acceleration response under analysis.

On the other hand, the expression developed by Arias (Arias 1970) to establish the intensity of an acceleration time history is:

$$I_{A} = \frac{\pi}{2g} \int_{0}^{T_{t}} [a(t)]^{2} dt$$
 [4]

Due to the mathematical similarity between expressions [3] and [4], and considering that the Arias Intensity is a well-known parameter, it is proposed to use the Arias Intensity to evaluate the energy of the acceleration responses of the SDOF of different natural frequencies. With this simple procedure, the Arias Spectrum is introduced as a complementary method to estimate the predominant frequency of an acceleration time history.

Figure 11 shows two examples of the effectiveness of Arias Spectrum for assessing the predominant period of acceleration records. The two stations recorded the Maule Earthquake with peak accelerations greater than 0.5g.

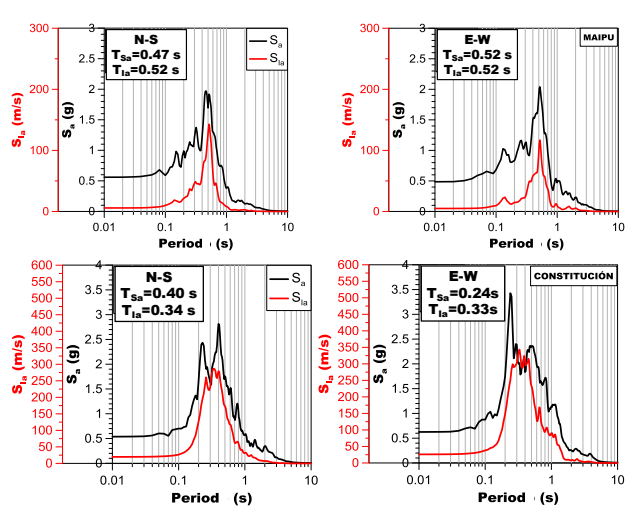


Figure 11. Response spectra and Arias Intensity spectra of the recorded accelerations at Maipu and Constitucion.

Figure 11a shows the Arias Spectrum (red line identified as  $S_{la}$ ) and the elastic pseudo-acceleration response spectra (5% of damping) of the two components recorded on Maipu seismic station (black line identified as  $S_a$ ). As can be seen, the Arias Spectrum shows the same period where the response is clearly amplified, suggesting that this period can be considered as the predominant period of the site.

Figure 11b presents the case of Constitucion station. In this case, the response spectra show the maximum amplifications at periods of 0.40 and 0.24 s, for the N-S and E-W components, respectively. However, the Arias

Spectra of each component are practically the same, 0.33 and 0.34 s, values that likely correspond to the predominant period of the site.

Consequently, in each site where the Maule Earthquake was recorded, the predominant period was obtained using the information provided by the response spectra and the Arias Intensity.

A similar analysis was carried out with the available information of each seismic station that recorded the Illapel Earthquake. As an example, the data obtained at station C180 are presented in Figure 12, where the HVSR using the microtremors recorded in the station and the response spectra and the Arias Intensity spectra of the Illapel Earthquake are plotted.

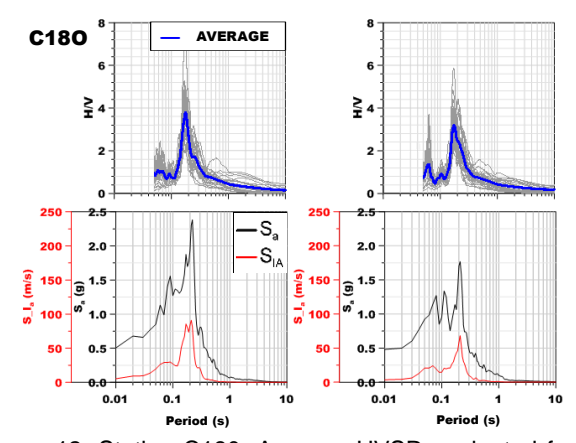


Figure 12. Station C180. Average HVSR evaluated from microtremors recorded in the station (upper plots). Response spectra and Arias Intensity Spectra (lower plots).

In Figure 13 the predominant periods of the site against the predominant periods evaluated independently from ambient vibrations (stations of Maule Earthquake) and microtremors (stations of Illapel Earthquake) are plotted.

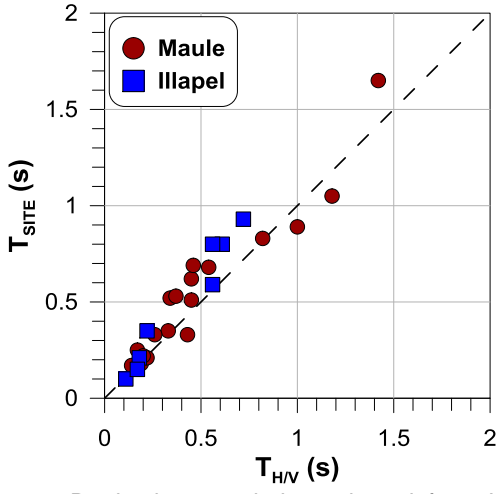


Figure 13. Predominant periods evaluated from HVSR,  $T_{H/V}$ , and from the response and Arias Intensity spectra,  $T_{\text{site.}}$ 

These results indicate a fairly good agreement between both values, suggesting that the HVSR is a good procedure for evaluating the predominant period of a site, or the period where the response spectra would tend to present the maximum amplification.

It is important to mention that there are a significant number of publications reporting the development of nonlinear site amplification when the shaking is sufficiently strong (Kokusho 2004; Noguchi et al, 2008; Régnier et al. 2017). In this context, it is apparent that the level of strains involved in the HVSR is radically smaller than the strain level induced by strong motions as the case of Maule and Illapel Earthquakes. However, the presented data suggest that the predominant period is not seriously affected by the strain level induced by the shaking. This fact could be explained by the results reported by Choi et al. (2005), who concluded that the nonlinearity of amplification factors is significant for sites with  $V_{S30}$  < 180 m/s, but relatively small for sites with  $V_{S30} > 300$  m/s. In this respect, none of the Chilean sites that have been analyzed presented V<sub>S30</sub> smaller than 210 m/s, and most of them are characterized with a value greater than 350 m/s.

### 7 SITES WITH A DIFFUSE PREDOMINANT PERIOD

There are sites that do not show a clear predominant period. These sites are associated with geotechnical conditions of high stiffness, so the impedance between the soil and bedrock is not relevant. Thus, the amplification is low and it takes place in a broad band of frequencies. The acceleration time histories recorded in the station San Jose during the Maule Earthquake show this type of response. Figure 14 shows a plot of the resulting pseudo-acceleration response spectra of both horizontal components. In particular the E-W component develops several periods where the response is amplified, in the range of 0.1 to 0.5 seconds.

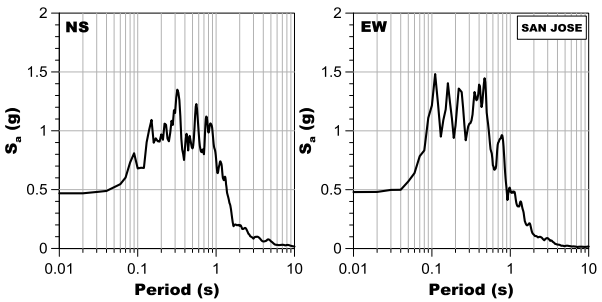


Figure 14. Pseudo-acceleration response spectra computed from recorded accelerations of the Maule Earthquake in San Jose station.

Moreover, the HVSR also confirm the existence of sites with a diffuse predominant period. Figure 15 shows four typical different shapes of HVSR obtained by means of ambient vibrations in Santiago (Vergara et al. 2016). Shape 1, commonly associated with soft soils, shows a clear peak that permits the identification of the predominant period of the site. Shape 2, associated with medium to soft soils, also shows a clear peak, but its amplitude is rather low, less than 3 - 4. Shapes 3 and 4

are basically flat, showing no amplification. These flat shapes of the HVSR are associated with very stiff soil deposits such as the Santiago gravel, with shear wave velocity greater than 700 m/s (Pastén et al. 2016).

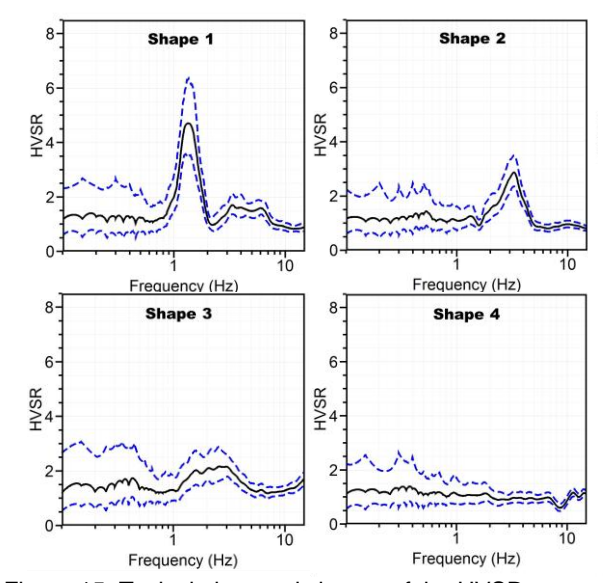


Figure 15. Typical observed shapes of the HVSR

Therefore, it can be concluded that when a flat shape of the HVSR is obtained, the site corresponds to a stiff material, where the seismic amplification is reduced in comparison with others sites. This is an important practical fact, because it makes possible the identification of those sites that are not conflicted from the point of view of their seismic response.

# 8 EQUIVALENT SHEAR WAVE VELOCITY, V<sub>S30-E</sub>

The current shear wave velocity of the upper 30 m, V<sub>S30</sub>, corresponds to the shear wave velocity that reproduces the same propagation time of the actual upper 30 m of the graound. This implies that the sequence of different soil layers does not affect the value of V<sub>S30</sub>. However, the seismic response at the ground surface can be strongly affected by the sequence of the soil layers. For example, Figure 16 presents the transfer function base-surface of two stratigraphic profiles, with identical V<sub>S30</sub>, both including a soft 10 m-thick layer with Vs = 150 m/s. In the profile of Figure 16a, the soft layer is on the surface, while in the profile of Figure 16b, the soft layer is located at a depth of 20 m. It can be seen that when the soft layer is located below the layer of Vs = 550 m/s, it practically acts as a seismic isolator, while at the surface it amplifies the response due to the large impedance.

This simple example shows that  $V_{\rm S30}$  is not a good parameter because it does not take into account the order or sequence of the layers that may exist in the upper 30 m of a site. To overcome this situation, it is proposed to use an equivalent shear wave velocity that reproduces the same stiffness of the actual top 30 m of the site. Instead of using for the top 30 m of the site, a shear wave velocity that has the same time of traveling throughout this 30 m, it

is proposed to use a shear wave velocity that reproduces the same fundamental period of the isolated upper 30 m of the ground.

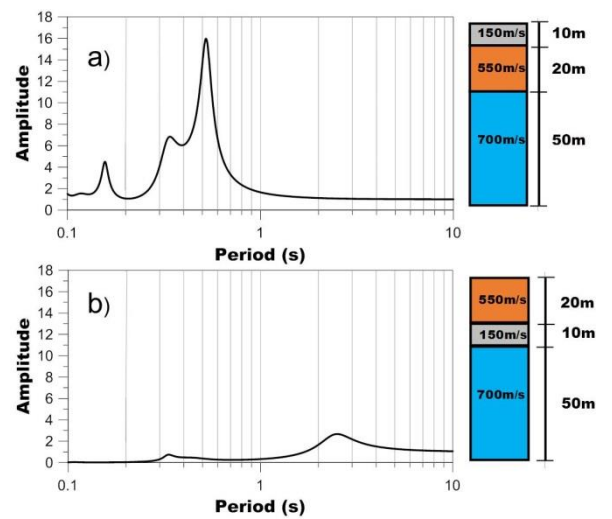


Figure 16. Transfer functions of two soil profiles with identical  $V_{\rm S30}$  and different sequence of layers.

Knowing the stratigraphy of the top 30 m of a site, in terms of the sequence of layers, thickness and shear wave velocity of each layer, the theoretical fundamental period,  $T_{F-30}$ , of the isolated top 30 m, can be computed numerically, using for instance, the 1D equivalent linear analysis. Then, the evaluation of the equivalent shear wave velocity,  $V_{S30-E}$ , is straightforward using the well-known expression of the fundamental period of a single stratum of 30 m in thickness:

$$V_{S30-E} = \frac{120}{T_{F-30}}$$
 [5]

The capability of  $V_{\rm S30-E}$  for assessing the seismic response of layered grounds has been checked by means of 1D analyses considering different complex soil stratigraphy. Three different soil layers in the upper 30 m of a rather deep site have been considered. Each layer has the same thickness of 10 m and shear wave velocities of 100, 200 and 500 m/s. Below 30 m, a soil with a shear wave velocity of 850 m/s and 100 m in thickness has been included. For six different combinations of the three upper soil layers, Figure 17 shows the resulting theoretical transfer functions when the current  $V_{\rm S30}$ , the proposed  $V_{\rm S30-E}$  and the actual layered soil structure, are used in the numerical analyses.

The same analyses were repeated considering the soil below 30 m to have a shear wave velocity of 300 m/s. The results are presented in Figure 18.

The different sequences of the three upper soil layers have the same value of  $V_{\rm S30}$ , accordingly, the same transfer function is obtained. However, each sequence has its own seismic response and therefore, a different transfer function. For the first mode, the proposed equivalent shear wave velocity is in good agreement with

the different transfer functions of each of the analyzed stratigraphy.

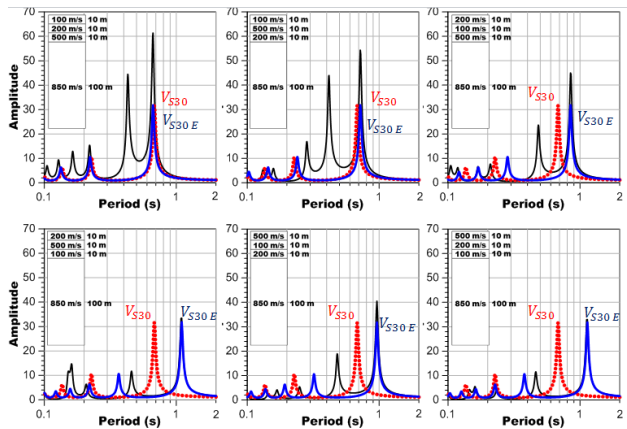


Figure 17. Transfer functions considering in top 30 m the current  $V_{S30}$  (in red), the proposed  $V_{S30-E}$  (in blue) and the actual stratigraphy (in black).

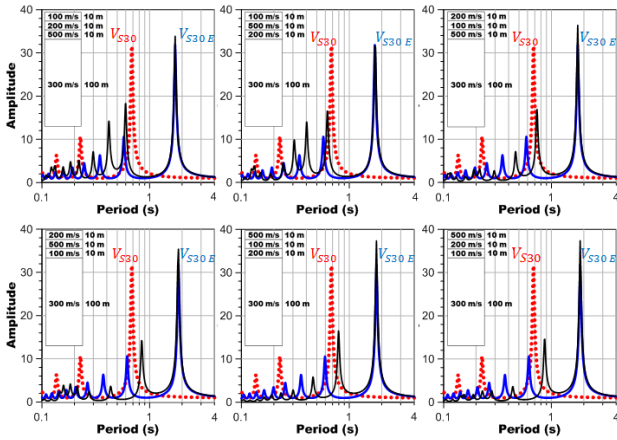


Figure 18. Transfer functions considering in top 30 m the current  $V_{S30}$  (in red), the proposed  $V_{S30-E}$  (in blue) and the actual stratigraphy (in black).

# 9 PROPOSED SITE CLASSIFICATION

A fundamental observation is associated with the fact that during large or mega-earthquakes, rigid soil deposits, such as rock outcrops, cemented soils or very dense gravels, have shown a significant reduction in the number of damaged structures, even cases of no damage have been reported on these type of sites. On the other hand, soft soil deposits, as for example, the clayey material of Mexico City, or the bay mud of San Francisco, or the sandy soils of Valparaíso, have shown a dramatic number of damaged structures as well as fully collapsed ones. With this strong and repeated empirical evidence, the seismic site classification must be able to identify and group appropriately the different sites according to similar seismic behavior.

The best seismic behavior has been observed in rock outcrops. Therefore, the best material in site characterization has to be massive rock (Site Class A),

which can be characterized simply by a shear wave velocity greater than 800 m/s in the top 30 m.

It is considered that soil deposits with a high rigidity are those with a fundamental period smaller than 0.3 s and a shear wave velocity greater than 500 m/s. Therefore, a Site Class B is proposed, with properties  $V_{\rm S30-E} > 500 \text{m/s}$  and a predominant period obtained from HVSR,  $T_{\rm H/V} < 0.3 \, \text{s}$ , or flat HVSR such as Shape 4 of Figure 15.

Site Class A and Site Class B are associated with sites that generate the lowest seismic demand when a large earthquake hits an area. The corresponding design spectra must reflect this condition.

To consider rigid sites, it is important to mention that very dense uncemented sandy soils, may in exceptional cases reach shear wave velocities close to 400 m/s at confining pressure less than 1 MPa. However, for the same level of pressure, common values of Vs for uncemented dense sandy soils are of the order 280 m/s. Therefore, a rigid site can be represented by shear wave velocities in the range of 300 to 500 m/s. In terms of fundamental period, a range between 0.3 to 0.5 s is suggested. Consequently, a Site Class C is proposed, with properties  $V_{\rm S30-E} > 300 {\rm m/s}$  and a predominant period obtained from HVSR,  $T_{\rm H/V} < 0.5$  s, or flat HVSR such as Shape 4 of Figure 15.

The following Site Class D is associated with medium to low rigidity soil deposits, which can be characterized by  $V_{S30-E} > 180$  m/s and a predominant period obtained from HVSR,  $T_{H/V} < 0.8$  s.

The softer classification corresponds to Site Class E, with  $V_{\text{S30-E}} < 180 \text{ m/s}.$ 

It is necessary to keep in mind that Site Class D and Site Class E are the most seismically demanding sites, and therefore, must be analyzed carefully.

Table 9 summarizes the proposed site classification. Site Class F is also included in order to group those sites with peculiar geological-geotechnical conditions that require special analyses, such as liquefiable soil, peats, quick clays, collapsible soils, expansive soils and saline soils.

Table 9. Proposed Seismic Site Classification

Site Class	General description	V <sub>S30-E</sub> (m/s)	T <sub>H/V</sub> (s)
Α	Rock	≥ 800	/
В	Very dense soils	≥ 500	< 0.30 (or flat)
С	Dense, firm soils	≥ 300	< 0.50 (or flat)
D	Medium-dense or medium-firm soils	≥ 180	< 0.80
E	Soft soils	< 180	/
F	Special soils	-	

The main parameter to classify a site is the equivalent shear wave velocity of the upper 30 m of the site,  $V_{\text{S30-E}}$ . Then, the predominant period,  $T_{\text{H/V}}$ , is an additional parameter that has to be used to confirm the Site Class. If the required predominant period is not satisfied, then, the resulting Site Class is degraded to the next Site Class.

Figure 19 shows the response spectra computed from the acceleration time histories recorded in two sites during the Maule Earthquake. The Concepción site consists of about 110 m of a sandy soil deposit with a shallow water table, whereas Peñalolen site consists of a non-saturated clayey soil of 24 m in thickness, below which dense gravel materials are encountered. The values of  $V_{\rm S30-E}$  obtained in Concepción and Peñalolen are 240 and 290 m/s, respectively. If shear wave velocities of the top 30 m are used alone, these sites should be classified as Site Class D. However, when the predominant periods are considered, the site of Concepción  $(T_{\rm H/V}=1.4~{\rm s})$  has to be modified, classifying as Site Class E. This site classification is in a good agreement with the actual observed spectra.

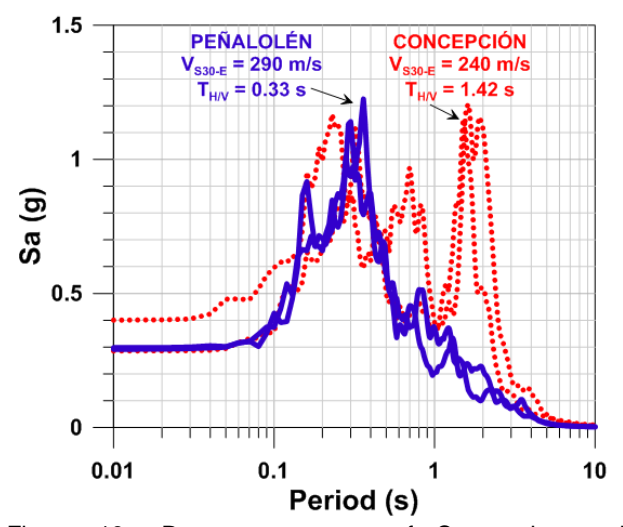


Figure 19.- Response spectra of Concepcion and Peñalolen sites, evaluated from records of Maule Earthquake.

### 10 CONCLUDING REMARKS

In spite of the advances in the field of earthquake engineering, economic losses left by large recent earthquakes are still considerable, far from any socioeconomically satisfactory standard. Modern society is wanting not only life protection but is also demanding that buildings can be immediately occupied after a strong earthquake. Historically, seismic design has been oriented to provide resistance to the structure elements. However, this approach has been shown to be insufficient to quarantee successful seismic behavior of structures. The new paradigm that would reduce the damage and losses resulting from an earthquake is the performance-based seismic design (PBSD). This design methodology allows engineers to design structures and nonstructural components with a desired seismic performance for a specified level of hazard. Accordingly, seismic design has moved from resistance criteria to performance objectives that have to be satisfied by the structure during and after earthquakes.

This design methodology requires a high standard in the different items that control the seismic analysis. One of the key factors is associated with the seismic loads. which are strongly dependent on the local ground conditions. The current Site Classifications used in different seismic countries have several flaws, which this paper has identified and attempted to improve.

Acceleration time histories recorded during the Maule Earthquake (Mw=8.8) and Illapel Earthquake (Mw=8.3) were analyses in terms of their pseudo-acceleration response spectra. To identify the predominant period of each station a complementary tool is proposed; the Arias Intensity Spectrum. It corresponds to the Arias Intensity of the acceleration response of each SDOF. This means that each considered frequency has associated a value of its Arias Intensity. This spectrum tends to exalt in a better way the predominant frequency, or period, of the signal.

The analyses of the available data permitted confirm that the H/V spectral ratio obtained via ambient vibrations or microtremors, reproduces the predominant periods shown by the response spectra.

An alternative seismic site classification has been proposed, which incorporates two important dynamic parameters of the ground: the equivalent shear wave velocity,  $V_{\rm S30-E}$ , of the upper 30 m and the predominant period of the soil deposit. The  $V_{\rm S30-E}$  reproduces the dynamic lateral stiffness of the upper 30 m of the ground. It is proposed that the predominant period of the soil deposit be estimated via the H/V spectral ratio of ambient vibrations.

### **ACKNOWLEDGEMENTS**

The author wants to acknowledge the valuable help of Dr. Laurence Wesley and Dr. Felipe Ochoa. The strong collaboration provided by the colleagues of CMGI Ltda., Javiera Gonzalez, Guillermo Valladares, Loreto Vergara and Gustavo Peters is also gratefully acknowledged.

### REFERENCES

- Aon Benfield. 2015. 2015 Nepal Earthquake Event Recap Report. webpage at: impactforecasting.com.
- ASCE/SEI 7-10. 2013. Minimum Design Loads for Buildings and Other Structures. American Society of Civil Engineers. Third Printing, Revised commentary.
- Arias A. 1970. A Measure of Earthquake Intensity. R.J. Hansen, ed. Seismic Design for Nuclear Power Plants, MIT Press, pp. 438-483.
- Barrientos, S. 2015. Technical Report Illapel Earthquake. National Seismological Center, CSN (in Spanish).
- Borcherdt, R. 1970. Effect of Local Geology on Ground Motion near San Francisco Bay. Bulletin of Seismological Society of America. Vol. 60, No.1, pp. 29-61.
- Borcherdt R. 1994. Estimates of Site-Dependent Response Spectra for Design (Methodology and Justification). Earthquake Spectra. 10 (4), 617-653.
- Borcherdt, R. and Gibbs, J. 1976. Effects of Local Geological Conditions in the San Francisco Bay Region on Ground Motions and the Intensities of the 1906 Earthquake. Bulletin of the Seismological Society of America. Vol. 66, No. 2, pp. 467-500.

- Borcherdt, R. and Glassmoyer, G. 1992. On the Characteristics of Local Geology and their Influence on Ground Motions Generated by the Loma Prieta Earthquake in the San Francisco Bay Region, California. Bull. Seis. Soc. Am. 82, 603-641.
- Celebi, M. Prince J. Dietel C. Onate M. and Chavez G. 1987. The Culprit in Mexico City Amplification of Motions. Earthquake Spectra 3, 315-328.
- Cimellaro, G. 2017. New Trends on Resiliency, Proceedings 16th World Conference on Earthquake Engineering, Santiago, Chile.
- Choi, Y. Stewart J.P. 2005. Nonlinear Site Amplification as Function of 30 m Shear Wave Velocity. Earthquake Spectra 21, pp. 1-30.
- Dobry R. Borchert R. Crouse C. Idriss I. Joyner W. Martin G. Power M. Rinne E. and Seed R. 2000. New Site Coefficients and Site Classification System Used in Recent Building Seismic Code Provisions. Earthquake Spectra. 16(1), 41-67.
- DS 61. 2011. Decreto Supremo, Diseño Sísmico de Edificios. Diario Oficial de Chile. (In Spanish).
- Eurocode 8. 2004. Design of structures for earthquake resistance. European Committee for Standardization.
- FEMA. 2012. Seismic Performance Assessment of Buildings, Volume 1 Methodology.
- Henríquez, H. 1907. El Terremoto de Agosto bajo el Punto de Vista Constructivo.
- Horspool N. King A. Lin S. and Uma S. 2016. Damage and Losses to Residential Buildings during the Canterbury Earthquake Sequence. NZSEE Conf.
- Indirli, M and Apablaza, S. 2010. Heritage Protection in Valparaiso (Chile): The "Mar Vasto" project. Revista Ingeniería de Construcción, Vol. 25, No.1.
- Kajitani Y. Chang S. and Tatano H. 2013. Economic Impacts of the 2011 Tohoku-Oki Earthquake and Tsunami. Earthquake Spectra. Vol. 29, No. S1, pp. S457-S478.
- Koller, M., J.-L. Chatelain, B. Guiller, A.-M. Duval, K. Atakan, C. Lacave and P.-Y. Bard. 2004. Practical user guidelines and software for the implementation of the H/V ratio technique: measuring conditions, processing method and results interpretation. 13WCEE, Vancouver, Canada.
- Kokusho, T. 2004. Nonlinear Site Response and Strain-Dependent Soil Properties. Current Science, Vol. 87, No. 10, pp. 1363–1369.
- Konno, K. and T. Ohmachi. 1998. Ground-Motion characteristics estimated from spectral ratio between horizontal and vertical components of microtremor. Bull. Seism. Soc. Am., Vol. 88, pp. 228-241.
- Lachet, C. and P.Y. Bard. 1994. Numerical and theoretical investigations on the possibilities and limitations of Nakamura's Technique", J. Phys. Earth, Vol. 42, pp. 377-397.
- Lermo, J. and J. Chávez-García. 1993. Site Effect Evaluation Using Spectral Ratios with Only One Station. Bull. Seism. Soc. Am., Vol. 83, No. 5, pp. 1574-1594.
- Montessus de Ballore. 1911. Seismic History of Southern Los Andes South of Parallel 16" (In Spanish), Cervantes Barcelona press, Santiago, Chile.

- Mohraz B. 1976. A Study of Earthquake Response Spectra for Different Geological Conditions. Bulletin of the Seismological Society of America. 66 (3), 915-935.
- Nakamura, Y. 1989. A Method for Dynamic Characteristics Estimation of Subsurface Using Microtremor on the Ground Surface. Quarterly Report of Railway Technical Research Institute (RTRI) 30:1, 25-33.
- Noguchi, S. and Sasatani, T. 2008. Quantification of Degree of Nonlinear Site Response. The 14WCEE, Beijing, China.
- Pastén, C. 2007. Seismic Response of Santiago Basin. Master Thesis Department of Civil Engineering, University of Chile. (in Spanish).
- Pastén, C. Sáez, M. Ruiz, S. Leyton, F. Salomón, J. and Poli, P. 2016. Deep characterization of the Santiago Basin using HVSR and Cross-Correlation of Ambient Seismic Noise. Engineering Geology 201, 57–66.
- Pitilakis K. Gazepis C. Anastasiadis A. 2004. Design Response Spectra and Soil Classification for Seismic Code Provisions. 13<sup>th</sup> WCEE. Vancouver, Canada.
- Priestley M.J.N. 2000. Performance Based Seismic Design. 12<sup>th</sup> WCEE.
- Régnier, J. Cadet, H. and Bard P-Y. 2017. Impact of non-Linear Soil Behavior on Site Response Amplitude. 16WCEE, Santiago, Chile.
- Rodriguez, A. and Gajardo, C. 1906. La catástrofe del 16 de agosto de 1906 en la República de Chile. National Library of Chile.
- Seed, H. B., Ugas C. and Lysmer J. 1976. Site-Dependent Spectra for Earthquake-Resistance Design. Bull. Seismological. Soc.of America. Vol. 66, No.1, 221-243.
- Seed, H.B. Romo M. Sun J. Jaime A. and Lysmer J.
  1988. The Mexico Earthquake of September 19, 1985
  Relationships Between Soil Conditions and Earthquake Ground Motions. Earthquake Spectra. Vol. 4, No. 4, pp. 687-729.
- Senplades. 2016. Evaluación de los Costos de Reconstrucción Sismo en Ecuador Abril 2016. Secretaría Nacional de Planificación y Desarrollo de Ecuador. (in Spanish).
- Singh S. Lermo J. Dominguez T. Ordaz M. Espinosa J. Mena E. and Quaas R. 1988. The Mexico Earthquake of September 19, 1985 A study of Amplification of Seismic Waves in the Valley of Mexico with Respect to a Hill Zone Site. Earthquake Spectra 4, 653-673.
- Towhata, I. 2016. Personal Communication.
- USGS. 2011. American Red Cross Multi-Disciplinary Team. 2011. Report on the 2010 Chilean Earthquake and Tsunami Response: U.S. Geological Survey Open-File Report 2011-1053. Available at: https://pubs.usgs.gov/of/2011/1053/.
- Verdugo, R. 2009. Amplification Phenomena Observed in Downhole Array Records Generated on a Subductive Environment. Physics of the Earth and Planetary Interiors 175, pp. 63–77.
- Verdugo, R. and Gonzalez, J. 2015. Liquefaction-induced ground damages during the 2010. Soil Dynamics and Earthquake Engineering, 79, pp. 280–295.

- Verdugo, R. and Pastén, C. 2008. Seismic Source and its Effect on Site Response Observed in Chilean Subductive Environment. 6<sup>th</sup> Int. Conf. on Case Histories in Geotechnical Engineering, Arlington. USA.
- Vergara, L. and Verdugo, R. 2016. Characteristics of the Grounds with Severely Damaged Buildings in the 27F Earthquake. IX Chilean Congress of Geotechnical Engineering. Valdivia. (in Spanish).
- Watanabe T. and Karzulovic J. 1960. The seismic Ground Motions of May, 1960 in Chile (in Spanish). Anales de la Facultad de Ciencias Físicas y Matemáticas, Vol. 17. Universidad de Chile.